Hierarchically porous and nitrogen, sulfur-codoped graphene-like microspheres as a high capacity anode for lithium ion batteries

Dongfei Sun,[ab] Juan Yang[a] and Xingbin Yan*[ac]

[a] Laboratory of Clean Energy Chemistry and Materials, Lanzhou Institute of Chemical Physics, Chinese Academy of Science, Lanzhou 730000, P. R. China

[b] Graduate University of Chinese Academy of Sciences, Beijing 100080, P. R. China

[c] State Key Laboratory of Solid Lubrication, Lanzhou Institute of Chemical Physics, Chinese Academy of Sciences, Lanzhou 730000, P. R. China

Experimental section

Preparation of Ni template

Powdery Ni microspheres were prepared by reducing the commercial nickel hydroxide microspheres which can be obtained from everywhere (Henan Kelong New Energy Co., Ltd.). Typically, Ni microspheres were obtained by calcining the powdery nickel hydroxide microspheres at 500 °C for 2 h in air, followed by reducing at 600 °C for 2 h in a hydrogen atmosphere.

Preparation of 3D NS-GSs

3D NS-GSs were prepared by a precursor-assisted chemical vapor deposition method. Typically, Ni microspheres (6 g) and poly(vinylpyrrolidone) (PVP)/$(NH_4)_2S_2O_8$ aqueous solution (5ml, the concentrations of PVP and $(NH_4)_2S_2O_8$ are 0.2 g/ml and 0.5 g/ml, respectively) were mixed uniformly. After been dried, the mixture was placed into a quartz tube and heated to 400 °C under Ar (100 sccm)/H_2 (100 sccm) atmosphere for 1 h, and subsequently the temperature was increased to 800 °C for 1 h under the same conditions. Then, the sample was cooled rapidly to room temperature. Finally, the as-obtained

graphene/Ni product was etched in HCl solution (1 mol L^{-1}) at 80 °C for 48 h to remove Ni, and followed by drying at 60 °C for 48 h to obtain 3D NS-GSs. For preparing 3D GSs, the same procedures were carried out just without adding $(NH_4)_2S_2O_8$. Furthermore, in order to investigate the influence of oxygen-containing group on the structure and performance of 3D GSs, another carbon source (polyethylene glycol, PEG) with high oxygen content was also used.

Structural characterizations

The morphology and microstructure of the as-prepared samples was investigated using a field-emission scanning electron microscope (FE-SEM, JSM-6701F), and a transmission electron microscope (TEM, Tecnai G20). The structure and composition of the samples was recorded using a micro-Raman spectroscopy (JY-HR800, the excitation wavelength of 532nm) and an X-ray diffraction (XRD, Philips X' Pert Pro). The surface chemical species of the as-prepared 3D NS-GSs sample were examined on a Perkin-Elmer PHI-5702 multifunctional X-ray photoelectron spectroscope (XPS, Physical Electronics, USA). Nitrogen adsorption-desorption isotherm measurements were performed on a Micrometitics ASAP 2020 volumetric adsorption analyzer at 77 K.

Electrochemical measurements

The working electrodes and lithium-ion half-cells were prepared as follows. Typically, a mixture of 85 wt% active material (3D GSs or 3D NS-GSs) and 15 wt% polyvinylidene difluoride (PVDF) was milled with N-methyl pyrrolidone (NMP) to form a homogeneous slurry, and the mixture was coated onto a copper foil. As-prepared working electrodes were dried under vacuum at 110 °C for 10 h. After being pressed, the electrodes were assembled into coin cells (CR2032) in an argon-filled glove box by using 1 mol L^{-1} $LiPF_6$ in dimethyl carbonate (DMC) and ethylene carbonate (EC) (1:1, v/v) as the electrolyte and pure lithium foil as the counter electrode. The assembled coin cells were tested in the voltage range of

0.01~3.0 V on a CT2001A cell test instrument (LAND Electronic Co.). All the electrochemical measurements were carried out at 25 °C in a digital biochemical incubator and the specific capacity was calculated based on the weight of each active material. Cyclic voltammetry (CV) (0.01~3 V, 0.01 mV s^{-1}) and electrochemical impedance spectroscopy (EIS) measurements were carried out on a CHI 660D electrochemical workstation.

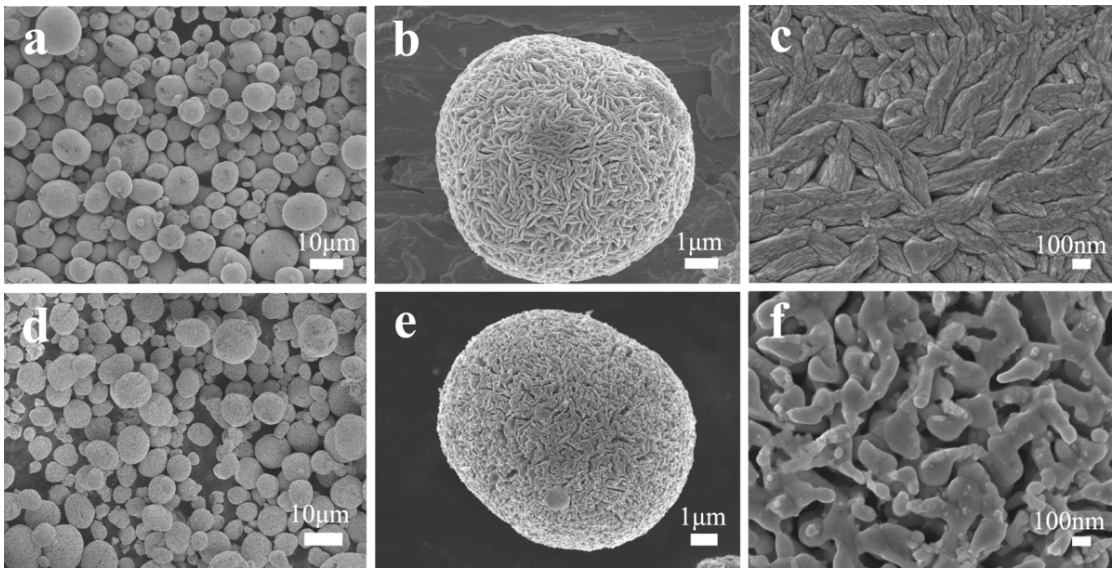

Fig. S1 (a-c) SEM images of nickel hydroxide microspheres and (d-f) nickel microspheres.

The Ni microspheres maintain the spherical structure, and each Ni microsphere consists of Ni nanoparticles with many pores, which forms a continuous and irregular porous structure in the micropheres. The porous structure can ensuing that liquid precursor are easily filled in the interstices of the Ni microspheres, meanwhile, the liquid precursor can prevent the agglomeration or deformation of the porous Ni microspheres at the CVD process.

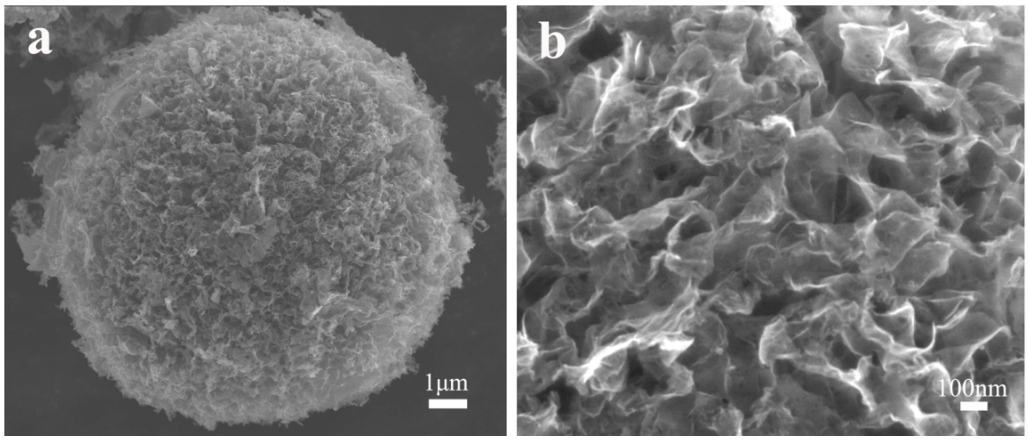

Fig. S2 (a) and (b) SEM images of 3D GSs.

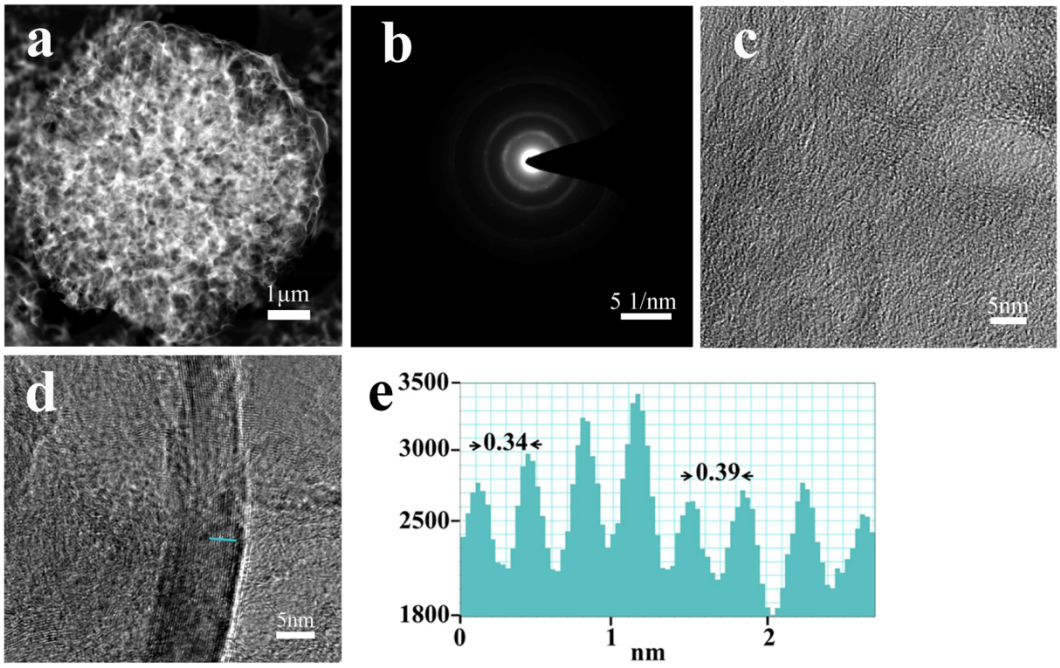

Fig. S3 (a) The dark-TEM image of a NS-GS, (b) SAED pattern of 3D NS-GSs, (c) and (d) higher magnification TEM images of 3D NS-GSs, and (e) the line profiles (extracted from (d)) of the d-spacing of graphene sheets.

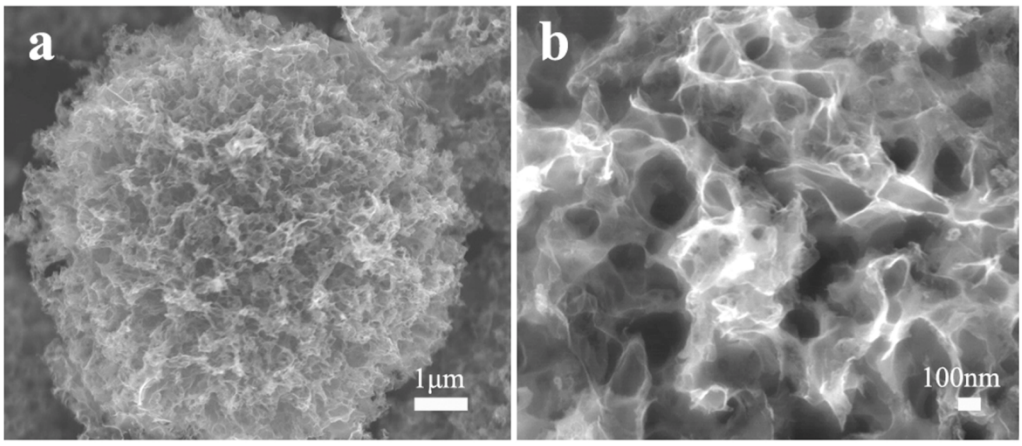

Fig. S4 (a) and (b) SEM images of 3D GSs (PEG as the carbon source).

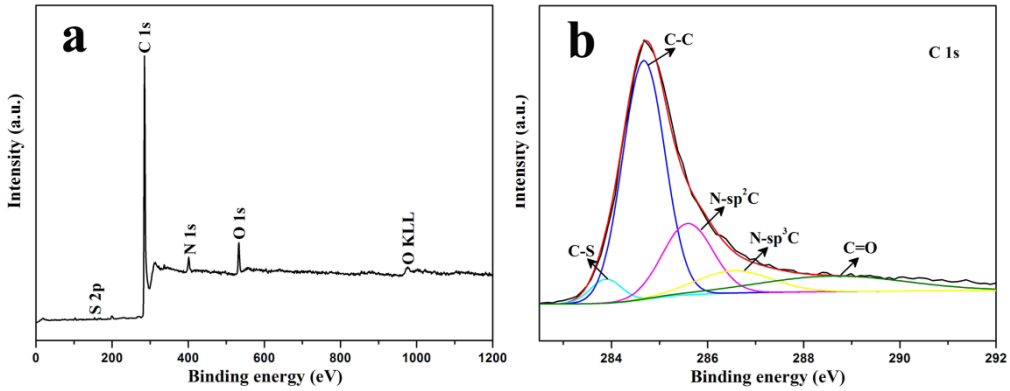

Fig. S5 (a) XPS and (b) C1s XPS spectra of 3D NS-GSs. Four components represent C-S, C-C, N-sp^2C, N-sp^3C and C=O, respectively.

Tab. S1. Structure and electrochemical properties of 3D GSs based on different carbon sources.

Materials (carbon source)	**C/O ratio**	**Reversible capacity (0.1 A g^{-1})**	**Surface area (m^2 g^{-1})**
3D GSs (PVP)	3.62	568	398
3D GSs (PEG)	17.51	587	434

In order to investigate the influence of structure and electrochemical properties of 3D GSs with different oxygen contents, the C/O ratio, reversible capacity, and surface area have been measured, as shown in Tab. S1. When PEG as the carbon source, the 3D GSs with a high oxygen content (C/O ratio is 17.51) are obtained. These graphene-like microspheres materials show a reversible capacity of 568 and 587 mAh g^{-1}, respectively. The results indicated that the oxygen content has little influence on both the structure and the electrochemical performance of the graphene-like microspheres.

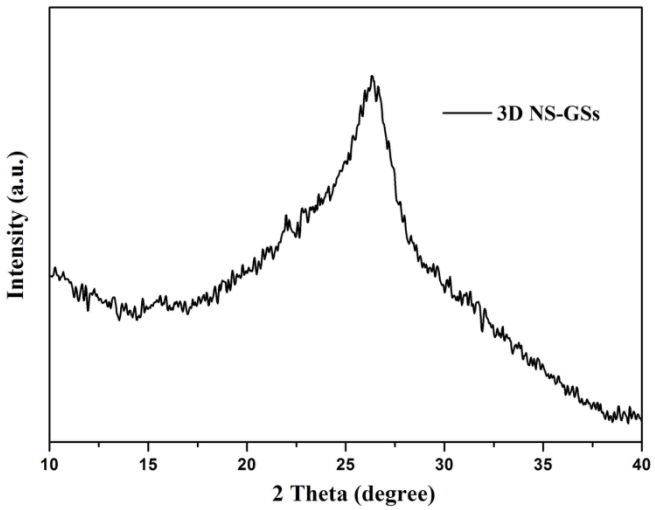

Fig. S6 XRD pattern of 3D NS-GSs.

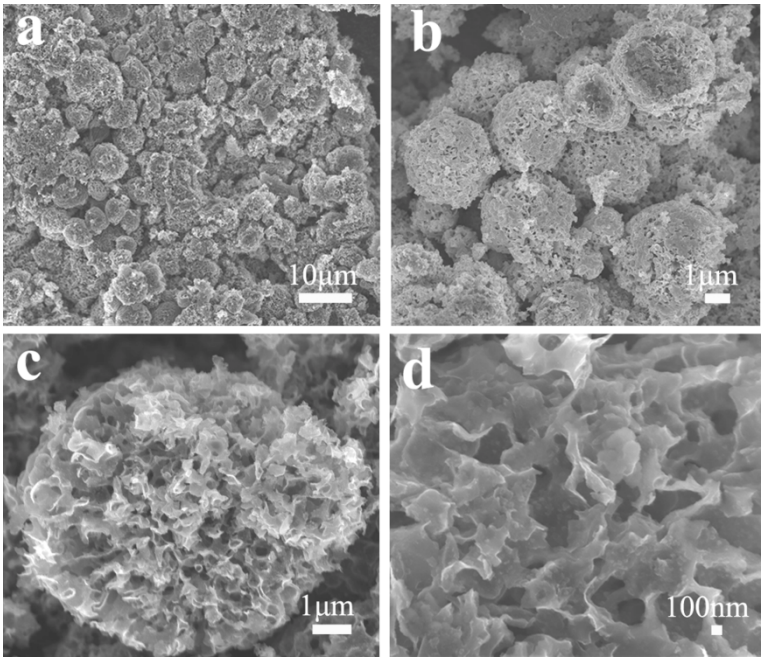

Fig. S7 SEM images of 3D NS-GSs electrode after 80th cycles.

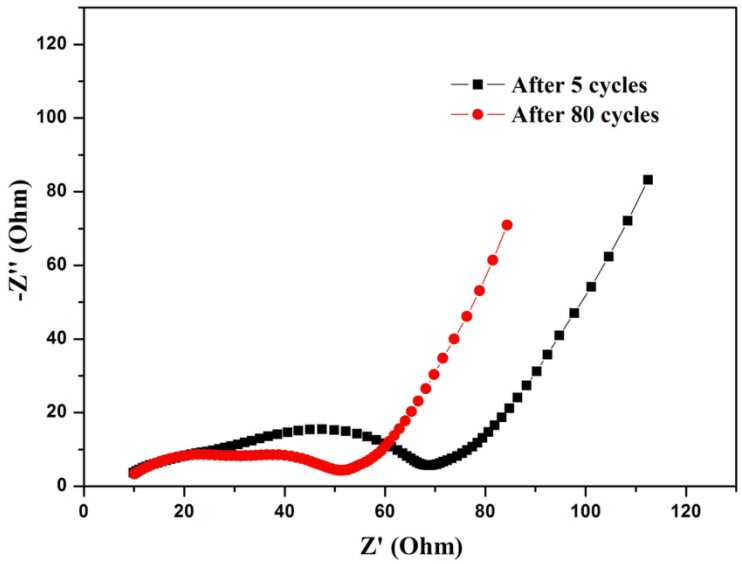

Fig. S8 Nyquist plots of the 3D NS-GSs electrode after 5th and 80th cycles at the current density of 0.1 A g^{-1}.

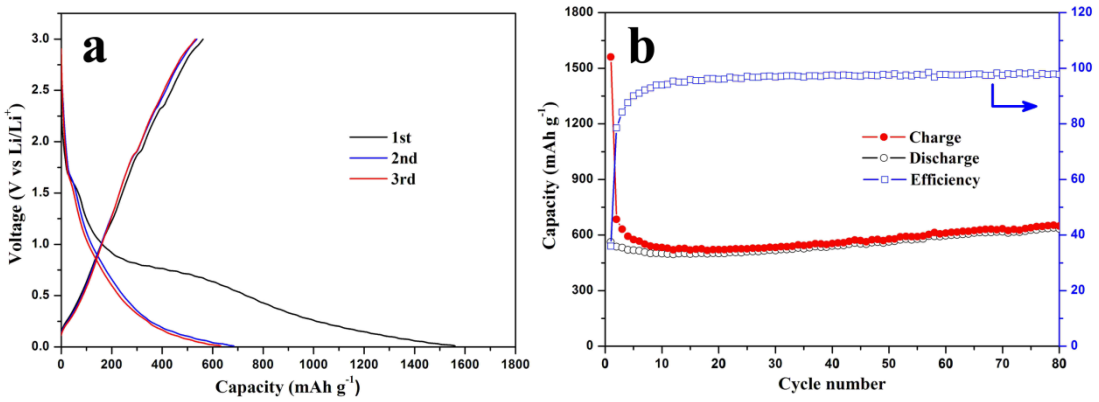

Fig. S9 (a) Galvanostatic charge-discharge voltage versus capacity profiles of the 3D GSs electrode at a current density of 0.1 A g^{-1}, and (b) cycling performance and Columbic efficiency of the 3D GSs electrode at 0.1 A g^{-1}.

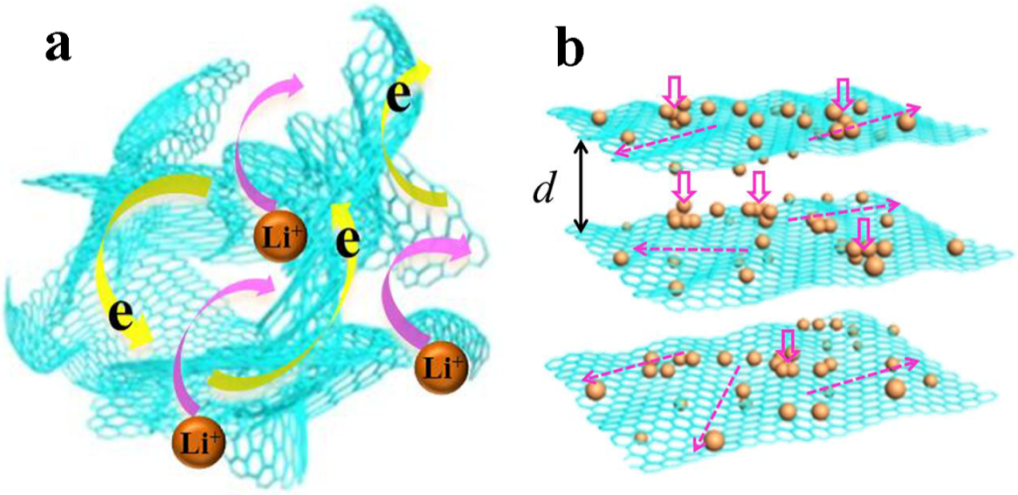

Fig. S10 Schematics of proposed Li diffusion mechanism through the pores and defects on (a) the graphene network and (b) the basal graphene plane of 3D NS-GSs. Yellow arrows indicate electron transfer through the graphene network, pink glows represent Li ion diffusion through the graphene network and the basal graphene plane. Notes and references

Tab. S2 Comparison of capacity and cycle performance for 3D NS-GSs anode with those of reported carbon anodes.

Typical examples	**Initial discharge capacity (0.1 A g^{-1})**	**Reversible capacity (0.1 A g^{-1})**	**Capacity after cycles (0.1 A g^{-1})**	**Capacity retention (%)**	**Ref.**
3D NS-GSs	**2438**	**1068**	**1112(80^{th})**	**104.5**	**this work**
N-doped graphene	2127 (0.05A/g)	1043	872(30^{th})	83.6	1
N-doped porous carbon	980	390	400(100^{th})	102.5	2
N-doped carbon xerogel	1480(0.1C)	645	665(50^{th})	103	3
S-doped graphene	1700(1C)	870	---	54.7 (4C, 500^{th})	4
N-doped carbon	1190(0.1C)	596	429(100^{th})	72	5

nanoparticles					
nitrogen-doped carbon spheres	1700 (0.05A/g)	816	660(50^{th})	80.8	6
mesoporous carbon	2385	1011	889(100^{th})	87.9	7

Notes and references

1 Z. S. Wu, W. C. Ren, L. Xu, F. Li and H. M. Cheng, *ACS Nano*, 2011, **5**, 5463-5471.

2 L. Wang, Y. L. Zheng, X. H. Wang, S. H. Chen, F. G. Xu, L. Zuo, J. F. Wu, L. L. Sun, Z. Li, H. Q. Hou and Y. H. Song, *ACS Appl. Mater. Interfaces*, 2014, **6**, 71170-7125.

3 X. C. Liu, S. M. Li, J. Mei, W. M. Lau, R. Mi, Y. C. Li, H. Liu and L. M. Liu, *J. Mater. Chem. A,* 2014, **2**, 14429-14438.

4 Y. S. Yun, V. D. Le, H. Kim, S. J. Chang, S. J. Baek, S. Park, B. H. Kim, Y. H. Kim, K. Kang and H. J. Jin, *J. Power Sources*, 2014, **262**, 79-85.

5 D. Bhattacharjya, H. Y. Park, M. S. Kim, H. S. Choi, S.. N. Inamdar and J. S. Yu, *Langmuir*, 2014, **30**, 318-324.

6 T. Q. Chen, L. K. Pan, T. A. J. Loh, D. H. C. Chua, Y. F. Yao, Q. Chen, D. S. Li, W. Qin and Z. Sun, *Dalton Trans.*, 2014, **43**, 14931-14935.

7 M. S. Kim, D. Bhattacharjya, B. Z. Fang, D. S. Yang, T. S. Bae and J. S. Yu, *Langmuir*, 2013, **29**, 6754-6761.